AD-A117 859 CAMBRIDGE UNIV (ENGLAND) CAVENDISH LAB F/G 20/4
REDUCTION OF AERODYNAMIC DRAG: TORSION DISC VISCOMETRY.(U)
JAN 82 W A WILBY, J E FIELD AFOSR-79-0057
UNCLASSIFIED AFOSR-TR-82-0619 NL

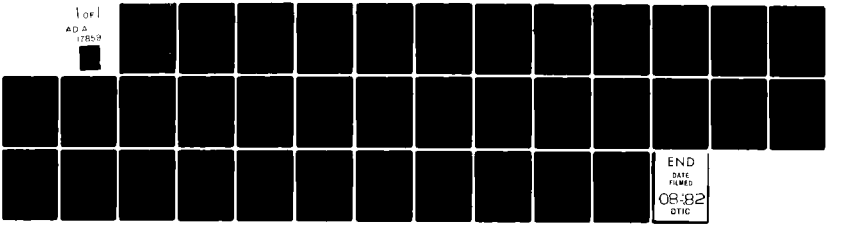

AFOSR-TR- 82-0619

(3)

UNIVERSITY OF CAMBRIDGE
DEPARTMENT OF PHYSICS

Interim Scientific Report:- May - December 1981

REDUCTION OF AERODYNAMIC DRAG:

TORSION DISC VISCOMETRY

Contract No. AFOSR-79-0057

W.A. Wilby

and

Dr. J.E. Field

Physics and Chemistry of Solids

Approved for public release; distribution unlimited.

Cavendish Laboratory, Madingley Road, Cambridge CB3 OHE.

Contents

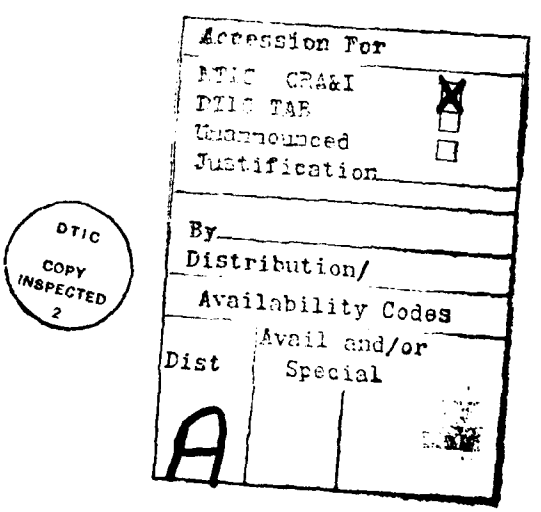

UNCLASSIFIED

SECURITY CLASSIFICATION OF THIS PAGE (When Data Entered)

REPORT DOCUMENTATION PAGE		READ INSTRUCTIONS BEFORE COMPLETING FORM
1. REPORT NUMBER AFOSR-TR- 82-0619	2. GOVT ACCESSION NO. AD-A117859	3. RECIPIENT'S CATALOG NUMBER
4. TITLE (and Subtitle) REDUCTION OF AERODYNAMIC DRAG: TORSION DISC VISCOMETRY		5. TYPE OF REPORT & PERIOD COVERED MAY 81 - DEC 81 INTERIM 6. PERFORMING ORG. REPORT NUMBER
7. AUTHOR(s) W A WILBY J E FIELD		8. CONTRACT OR GRANT NUMBER(s) AFOSR-79-0057
9. PERFORMING ORGANIZATION NAME AND ADDRESS CAVENDISH LABORATORY UNIVERSITY OF CAMBRIDGE CAMBRIDGE CB3 OHE, ENGLAND		10. PROGRAM ELEMENT, PROJECT, TASK AREA & WORK UNIT NUMBERS 61102F 2307/A2
11. CONTROLLING OFFICE NAME AND ADDRESS AIR FORCE OFFICE OF SCIENTIFIC RESEARCH/NA BOLLING AIR FORCE BASE, DC 20332		12. REPORT DATE JAN 82 13. NUMBER OF PAGES 34
14. MONITORING AGENCY NAME & ADDRESS (if different from Controlling Office)		15. SECURITY CLASS. (of this report) UNCLASSIFIED 15a. DECLASSIFICATION/DOWNGRADING SCHEDULE

16. DISTRIBUTION STATEMENT (of this Report)

Approved for public release; distribution unlimited.

17. DISTRIBUTION STATEMENT (of the abstract entered in Block 20, if different from Report)

18. SUPPLEMENTARY NOTES

19. KEY WORDS (Continue on reverse side if necessary and identify by block number)

AERODYNAMICS
BOUNDARY LAYERS
DRAG REDUCTION
TURBULENCE
RADIOACTIVITY
MOLECULAR AERODYNAMICS
VISCOMETER

20. ABSTRACT (Continue on reverse side if necessary and identify by block number)

This report describes the design, construction and evaluation of a working torsion disc viscometer. Initial tests at gas pressures between 9.1 mbar and 1000 mbar show that the theory of the instrument is adequate and that the viscometer is capable of detecting small changes in gas viscosity. A thorough investigation of the effect of radioactive irradiation on gas viscosity will be made shortly, following the work of Kestin and sHah (ref. 7). An analysis of their approach is given here, viewed in the light of our preliminary work, and

DD FORM 1 JAN 73 1473 EDITION OF 1 NOV 65 IS OBSOLETE

UNCLASSIFIED

SECURITY CLASSIFICATION OF THIS PAGE (When Data Entered)

suggests the most likely ways of achieving a change in gas viscosity.

Interim Scientific Report No. 3

1. Introduction

This report describes the design, construction and evaluation of a working torsion disc viscometer.

Initial tests at gas pressures between 0.1 mbar and 1000 mbar show that the theory of the instrument is adequate and that the viscometer is capable of detecting small changes in gas viscosity.

A thorough investigation of the effect of radioactive irradiation on gas viscosity will be made shortly, following the work of Kestin and Shah.

An analysis of their approach is given here, viewed in the light of our preliminary work, and suggests the most likely ways of achieving a change in gas viscosity.

2. Review of Work to Date

Kestin and Shah[7] (see also Clark, Kestin and Shah[1]) made an experimental investigation of the changes, caused by ionisation, in the apparent viscosities of various gases. They used a torsion disc viscometer to measure the viscosity and radioactive sources to produce ionisation of the gas. The changes in apparent viscosity were generally small, the most significant being decreases of 0.25 % and 7.6 % for air at 1 atmosphere and 1 mm Hg pressure respectively, and an increase of 5.25% for argon at 1 atmosphere.

To investigate the possibility of changing viscosity under flight conditions, we constructed an aerodynamic skin friction drag balance, which could measure the drag on a flat plate for air flows of up to 200 m/s at atmospheric pressure. High accuracy ($\sim$ 0.1%) was achieved at high speeds, but no changes in drag on irradiation were observed. At low speeds the accuracy is limited due to the small drag forces (down to 0.1 gf) and these errors were greater than or comparable with the magnitude of the change expected[2,4,15].

Accordingly we decided to make our own measurements on almost static gases using a viscometer giving higher accuracies than the drag balance.

The type of viscometer chosen was the torsion disc viscometer with a free disc suspended from a fine torsion wire (figure 1). This is simpler than rotating cylinder or fixed disc types, and is easier to use when making an extended series of measurements under different conditions.

It was also the same choice as made by Kestin and Shah, although our approach makes the use of the viscometer rather more straightforward.

3. Theory

Consider a circular disc of finite but small thickness (i.e. $h << R$), immersed in a fluid of density ρ and viscosity μ and suspended from a thin torsion wire giving a restoring force $\lambda\theta$.

If the disc is set oscillating the amplitude will be damped by the viscous action of the fluid (the wire will also contribute to the damping. this is considered later).

The equation of motion of the disc can be written

$$I\ddot{\theta} + D(\theta,\dot{\theta}) + \lambda\theta = 0$$

where the damping is some function of $\theta,\dot{\theta}$ and the properties of the fluid. If the damping is small ($D(\theta) << \lambda$) and roughly $\alpha\dot{\theta}$ (fluid velocity small) the motion will approximate to a damped simple harmonic motion.

Writing

$$I\ddot{\theta} + D\dot{\theta} + \lambda\theta = 0 \qquad (1)$$

the damping can be characterised by the logarithmic decrement of the system

$$\Delta = \ln\left(\frac{\theta n}{\theta n+1}\right) = \frac{DT}{2I} \qquad (2)$$

where

$$T = \frac{2\pi}{\omega} = 2\pi\sqrt{\frac{I}{\lambda}}$$

An experimental determination of Δ will therefore give us information on the fluid provided we can find an expression for D.

(An expression for T can easily be found in terms of the properties of the suspension wire -

According to Landau and Lifshitz[8] the restoring couple for a rod twisted about the axis of symmetry parallel to its length is

$$\frac{C\theta}{\ell} \quad \text{where} \quad C = \tfrac{1}{2} S\pi r_w^4 \tag{3}$$

The shear modulus S is related to the Young's Modulus and Poisson ratio by

$$S = \frac{E}{2(1+\sigma)} \tag{4}$$

and this leads to

$$T_o = 16\sqrt{\frac{\pi(1+\sigma)I1}{Ed^4}} \tag{5}$$

for the natural period.

The period with damping , T, is given by

$$T = T_o \sqrt{1 + (\tfrac{\Delta}{2\pi})^2} \simeq T_o \left(1 + \tfrac{1}{2} (\tfrac{\Delta}{2\pi})^2\right) \tag{6}$$

for simple harmonic motion).

To find an expression for D we need to solve the equations of motion of the fluid around the disc. The Navier Stokes equations take the following form in cylindrical polar coordinates (neglecting pressure gradients and assuming that the motion is cylindrically symmetric, valid assumptions for small damping after the decay of any transients).

$$\frac{\partial U_r}{\partial r} + \frac{U_r}{r} + \frac{\partial U_z}{\partial z} = 0 \qquad \text{(continuity)} \tag{7a}$$

$$\rho\left[\frac{\partial U_r}{\partial t} + U_r \frac{\partial U_r}{\partial r} + U_z \frac{\partial U_r}{\partial Z} - \frac{U_\phi^2}{r}\right] = \mu\left[\frac{\partial^2 U_r}{\partial r^2} + \frac{1}{r}\frac{\partial U_r}{\partial r} - \frac{U_r}{r^2} + \frac{\partial^2 U_r}{\partial z^2}\right] \tag{7b}$$

$$\rho\left[\frac{\partial U_\phi}{\partial t} + U_r \frac{\partial U_\phi}{\partial r} + \frac{U_r U_\phi}{r} + U_z \frac{\partial U_\phi}{\partial z}\right] = \mu\left[\frac{\partial^2 U_\phi}{\partial r^2} + \frac{1}{r}\frac{\partial U_\phi}{\partial r} - \frac{U_\phi}{r^2} + \frac{\partial^2 U_\phi}{\partial z^2}\right] \tag{7c}$$

$$\rho\left[\frac{\partial U_z}{\partial t} + Ur\frac{\partial U_z}{\partial r} + U_z\frac{\partial U_z}{\partial z}\right] = \mu\left[\frac{\partial^2 U_z}{\partial r^2} + \frac{1}{r}\frac{\partial U_z}{\partial r} + \frac{\partial^2 U_z}{\partial z^2}\right] \tag{7d}$$

The presence of the non linear terms make a solution difficult. However, to get an idea of the type of motion let us suppose that U_r and U_z are small and that

$$U_\phi \to 0 \text{ as } z,r \to \infty$$

$$U_\phi(z=\pm\frac{h}{2}, r<R) = r\omega\theta_o\cos\omega t = U_o\cos\omega t$$

i.e. we neglect the damping intially; θ_o is the amplitude of the motion. The equations then reduce to

$$\rho\frac{\partial U_\phi}{\partial t} = \mu\left(\frac{\partial^2 U_\phi}{\partial r^2} + \frac{1}{r}\frac{\partial U_\phi}{\partial r} - \frac{U_\phi}{r^2} + \frac{\partial^2 U_\phi}{\partial z^2}\right) \tag{8}$$

Near the surface of the disc

$$U_\phi \overset{\sim}{\propto} r\omega\cos\omega t$$

and so

$$\frac{\partial^2 U_\phi}{\partial r^2} + \frac{1}{r}\frac{\partial U_\phi}{\partial r} - \frac{U_\phi}{r^2} \simeq 0$$

suggesting that in the region of the disc a reasonable approximation to the equation of motion is

$$\rho\frac{\partial U_\phi}{\partial t} = \mu\frac{\partial^2 U_\phi}{\partial z^2} \tag{9}$$

or

$$\frac{\partial U_\phi}{\partial t} = \nu\frac{\partial^2 U_\phi}{\partial z^2}$$

This linear equation can be readily solved by the separation of variables (equivalent to Stokes 2nd problem[13]):- restricting our attention to the top of the disc, taking z=o on the surface for simplicity, we put $U_\phi \propto f(t)g(z)$ to get

$$\frac{1}{f}\frac{df}{dt} = \nu\frac{1}{g}\frac{d^2g}{dz^2} = \Omega \text{ where } \Omega \text{ is some complex constant.}$$

Then $f = e^{\Omega t}$, $g = e^{\sqrt{\frac{\Omega}{\nu}}z}$ neglecting the arbitrary multiplicative constants for the moment.

To fit the boundary conditions at the disc we put $\Omega = i\omega$

then $\sqrt{\frac{\Omega}{\nu}} = \pm\sqrt{\frac{\omega}{2\nu}}\,(1+i)$

Rejecting the +ve root to match the boundary condition at ∞ we get

$$V \propto e^{i\omega t} e^{-\sqrt{\frac{\omega}{2\nu}}\,(1+i)z}$$

or, taking the real part

$$V = r\omega\theta\cos\,(\omega t - z/\lambda) e^{-z/\lambda} \tag{10}$$

where $\lambda = \sqrt{\frac{2\nu}{\omega}} = \sqrt{\frac{\mu T}{\pi\rho}}$ is the penetration depth.

The solution takes the form of an oscillation, damped in the z direction, so that the region of interest is within a few λ of the disc.

The surface shear stress at the disc is given by

$$\tau = \mu \frac{\partial U}{\partial z}\phi\Big|_{z=o} = \frac{\theta_o \mu r \omega}{\lambda}\,(\sin\omega t - \cos\omega t) \tag{11}$$

$$\approx \frac{\mu r}{\lambda}\,(\omega\theta - \dot{\theta})$$

The term in θ can be thought of as effectively increasing the inertia of the disc, due to the fluid carred by the disc. For small damping, this can be neglected and our expression for the total damping is

$$D = 2\int_o^R \frac{\mu}{\lambda}\, 2\pi\, r^3 dr \qquad \text{(2 sides)}$$

Including a correction for the edge, assuming a similar equation of motion, we get

$$D = \pi R^4 \sqrt{\frac{\mu\omega\rho}{2}}\,(1 + \frac{2h}{R})$$

and the logarithmic decrement is thus

$$\Delta = \frac{\pi R^4 \sqrt{\pi\mu\rho T}}{2I}\,(1 + \frac{2h}{R}) \tag{12}$$

The damping due to the wire, Δ_o, can simply be added to this expression to get the total damping, provided Δ_o is small.

This expression is in agreement with measured drags for our viscometer to within a factor of 1.5 or so, underestimating the actual damping.

The major part of the discrepancy can be attributed to the effect of the edge of the disc.

A better expression has been obtained by Maries & van Paemel[10]. Writing $U_\phi = r\dot{\psi}(r,z,t)$ where ψ is the angular amplitude of the fluid, they solve the simplified Navier Stokes equation.

$$\frac{\partial \dot{\psi}}{\partial t} = \nu\left(\frac{\partial^2 \dot{\psi}}{\partial r^2} + \frac{3}{r}\frac{\partial \dot{\psi}}{\partial r} + \frac{\partial^2 \dot{\psi}}{\partial z^2}\right) \tag{13}$$

with the boundary conditions.

$\psi(t) = \theta(t) = \theta(0)e^{\Omega t}$ on the surface of the disc and $\psi(z, r \to \infty) = 0$. The time dependence is assumed to be as for damped SHM, i.e. $\Omega = i\omega - \Delta/T$.

The solution for the damping can be pieced together by considering different regions of the fluid in turn.

Near the edge (region 1 of figure 1) it can be assumed there is no z dependence, and using the time dependence this gives

$$\frac{d^2\psi_1}{dr^2} + \frac{3}{r}\frac{d\psi_1}{dr} + p^2\psi_1 = 0 \tag{14}$$

where $p^2 = -\frac{\Omega}{\nu}$.

writing $\psi = \frac{f(r)}{r}$ we see that

$$\frac{d^2 f}{dr^2} + \frac{1}{r}\frac{df}{dr} + \left(p^2 - \frac{1}{r^2}\right) f = 0$$

or, with $\rho = pr$

$$\frac{d\,f}{d\rho^2} + \frac{1}{\rho}\frac{df}{d\rho} + \left(1 - \frac{1}{\rho^2}\right) f = 0$$

which is Bessel's equation of order 1.

The solution for ψ_1 can therefore be expressed as a linear combination of first order Hankel functions of the first and second kind:-

$$\psi_1 = \frac{C_1 H_1^{(1)}(pr)}{r} + \frac{C_2 H_1^{(2)}(pr)}{r}$$

To meet the bondary conditions at ∞ and on the disc we need

$$\psi = \frac{\theta(t)\ R\ H_1^{(1)}(pr)}{rH_1^{(1)}(p_R)} \qquad (15)$$

Off the corner of the disc we can separate variables and use $\psi_2 = \psi_1$ for $z = h/2$ to get

$$\psi = \frac{\theta(t)e^{ip(z-h/2)}RH_1^{(1)}(pr)}{rH_1^{(1)}(pR)} \qquad (16)$$

Above the disc, assuming no r dependence, but allowing for the influence of the fluid in region 2, the equation of motion is

$$\frac{1}{\nu}\frac{\partial\psi_3}{\partial t} = \frac{\partial^2\psi_3}{\partial z^2} + \frac{4}{R}\left.\frac{\partial\psi_2}{\partial r}\right|_{r=R} \qquad (17)$$

With the identity [9]

$$\frac{dH_1^{(1)}(pr)}{dr} = -\frac{H_1^{(1)}(pr)}{r} + pH_o^{(1)}(pr)$$

this gives a differential equation in z which is readily solved to give

$$\psi_3 = \theta(t)\ \{1 - [2i(z-h/2)/R]\ [\frac{2}{pr} - H_o^{(1)}(pR)/H_1^{(1)}(pR)]\ \}\ e^{ip(z-h/2)}$$

Knowing ψ, the viscous torque on the disc can be calculated, and after some algebra, expanding the Hankel functions in their asymptotic series, Mariens and van Paemel get the following expression for the logarithmic decrement:-

$$\Delta = \frac{\pi R^4\sqrt{\pi\mu\rho T}}{2I}\left[1 + \frac{2h}{R} + \frac{\lambda}{R}\left(2 + \frac{3h}{R}\right) + \frac{3}{2}\left(\frac{\lambda}{R}\right)^2\left(1 + \frac{h}{4R}\right) + O\left(\left(\frac{\lambda}{R}\right)^4\right)\right] \qquad (19)$$

For small λ/R it can be seen that this reduces to our earlier expression.

The viscosity can be obtained from Δ by interation or by using a look-up chart.

Experimental data obtained by Mariens and van Paemel[10] and by Kestin and Wang[6] show that this equation generally gives values of μ correct to a few percent, entirely satisfactory for measurements of small viscosity changes.

A more accurate theoretical expression would undoubtedly be difficult to obtain, as centrifugal force must cause a radial motion of the fluid near the disc and consequent axial flow, i.e. U_r and U_z will not be negligible.

An approximate solution for the problem of a constantly rotating disc with U_r, $U_z \neq 0$ has been obtained (see Sparrow and Gregg[12] and Schlichting[11]) but not for the case of an oscillatory motion. However, adapting the results to an oscillating disc suggests a similar magnitude for Δ.

For $\lambda \gtrsim R$ our expression for Δ must break down due to the asymptotic expansion of the Hankel functions. This will happen for low gas pressures. An approximation to the solution can be obtained by solving equation 9 in a similar fashion to before, but with $u_\phi = o$ on the walls of the viscometer.

This gives

$$\Delta = \frac{\pi R^4 \mu T}{4I\lambda} \left[C(b_1/\lambda) + C(b_2/\lambda) + \frac{4h}{R} C(b_3/\lambda) \right] \qquad (20a)$$

where $$C(b) = \frac{\cosh(b/\lambda) \sinh(b/\lambda) + \cos(b/\lambda) \sin(b/\lambda)}{\sinh^2(b/\lambda) + \sin^2(b/\lambda)}$$

For large b/λ this reduces to equation 12 and for small b/λ reduces to

$$\Delta = \frac{\pi R^4 T \mu}{4I} \left(\frac{1}{b_1} + \frac{1}{b_2} + \frac{4h}{R} \frac{1}{b_3} \right) \qquad (20b)$$

This gives the correct dependance on μ, although the discrepancy between the magnitude of the measured drag and Δ calculated from 20b is rather worse than at high pressure. This is probably because the assumptions involved in equation 9 are unrealistic when $\lambda \sim R$; in particular the influence of the side walls of the viscometer is likely to be of great importance. An analysis of this problem will be made soon. However, the use of an equation of the form

$$\Delta = K\mu$$

where K is an empirically determined constant characteristic of the disc should be adequate for measuring changes in apparent viscosity at low pressure.

The approach used by Kestin and Shah in their work also involved an attempt to solve the simplified Navier-Stokes equation. Rather than assume the form of the time dependence, the Laplace transform was used to replace the time-dependence of the Navier Stokes equation and of the equation of motion of the disc. The viscous torque is constructed assuming that the torque is proportional to the torque calculated assuming the solutions for an infinite disc and an infinite cylinder. The "constant" of proportionality is an empirically determined function of the bondary layer thickness.

The resultant inverse Laplace transform cannot be solved exactly, but after some analysis the expression

$$\frac{3\pi\rho R^4 h}{I}\ C\left(\left(\frac{\delta}{R}\right)^2\right) + \frac{1}{\sqrt{2}}\left(1 + \frac{2h}{R}\right)\ \frac{1}{\sqrt{\Theta}}\left(1 - \frac{3}{2}\Delta - \frac{3}{8}\Delta^2\right)\frac{\pi\rho R^5}{I}\ C\left(\frac{\delta}{R}\right)$$

$$- 2\left(\frac{\Delta}{\Theta} - \Delta_o\right) = 0$$

where $\Theta = T/T_o$ and $\delta = \sqrt{\nu/\omega}$ was obtained by Kestin and Wang[6] and was used together with an empirically determined correction function by Kestin and Shah[7] to calculate apparent viscosities.

This proceedure warrants some criticism; firstly the viscosity only enters the problem through the correction function, which has values up to 3 for measurements at atomospheric pressure. This makes it hard to justify the use of such a complicated expression, with all its computational difficulties. Secondly, the equation does not approach the correct limit when δ/R is small.

We therefore feel that using the Mariens - van Paemel equation (19) and equation (20b) for $\lambda > R$ is a better approach. A possible further theoretical solution might be achieved by assuming the time dependence of the solution and Fourier or Laplace transforming wrt z. However, the inverse transform is again the difficult step (see ref. 3 for a general discussion of the problem).

4. Design

Having chosen the type of viscometer, the choice of disc and torsion wire material is critical. Initial studies led to a disc of several cm. diameter, with

a thickness of about 1mm. The wires used were restricted to those readily available, being either steel (piano wire) or CuBe, of $\sim$ 0.2 mm diameter.

Neither material showed any significant deterioration with time, and the restoring forces were accurately linear. The wire length used was generally between 10 and 20 cm. Some experiments with quartz fibres were made, but due to their brittleness these were not used. There were also doubts about their long term strength. This could be affected by water vapour for example. The chosen wire was fastened to the disc, and also suspended, by means of pinchucks.

To measure the angular position of the disc a small galvanometer mirror was fixed to the base of the lower pinchuck, just above the disc. The beam from a Spectra Physics 1 mW He/Ne laser was reflected from the mirror to a screen $\sim$ 2 m distant. The mirror was 5 mm in diameter with a focal length of 1 m. This gives a better spot on the screen than with a plane mirror; about 1 to 2 mm across typically. No sizeable amplitude errors are introduced by the curvature of the mirror provided the beam is central and the mirror is not too far from the axis of the rotation.

Starting the torsional motion in a consistent manner and without causing excessive non-axial vibration was a problem. This has been overcome by using an automatic starting system. This consists of a d.c. electric motor acting on the upper pinchuck. The motion is opposed by a spring, with a rigid stop defining an accurate zero position. A circuit has been built to give a preset number of pulses of the motor at the resonant frequency of the viscometer (figure 2). This gives a consistent starting amplitude and causes minimal other disturbance of the disc.

The disc is housed in a $\sim$ 6 mm thick glass cylinder of 18.3 cm internal diamter and 32 cm length. The ends have ground glass flanges which seal by "O" rings to 1 cm thick dural plates. The upper plate has gas tight lead throughs for a thermocouple and the starter motor. A hole in the plate connects to a Schaeritz PTD 310W pressure transducer, an Edwards Model 17 Pirani gauge and

the gas / vacuum lines. The lower plate is held by spring clips and is easily removed for the introduction of radioactive sources (figure 3). These are placed on the base and irradiate the underside of the disc. There is no need to alter the disc; this eliminates any change in calibration. The laser, screen and viscometer can be aligned accurately using the various reflected beams from the glass cylinder and galvanometer mirror.

The viscometer is contained in an insulating box having thick polystyrene sides and a polymethylmethacrylate (PMMA) front. The temperature can be controlled thermostatically (using light bulbs for heating) to an accuracy of $\pm$ 0.05°C.

To achieve maximum accuracy and ease of operation, we decided to measure the logarithmic decrement (log. dec.) automatically. Instead of measuring a series of amplitudes by eye, a circuit was built to count the number of oscillations, n, needed for the motion to decay to various known amplitudes. The log. dec. can then be obtained from the slope of a graph of $\ell n\theta$ versus n. Provided n (which is, of course, only accurate to the nearest integer) is large enough, the accuracy is good. By making four counts from an initial known amplitude, a five point graph is obtained. The log. dec. used is such that there are between 70 and 130 counts per section in normal use, giving an accuracy of $\sim$ 0.1 %. As this is comparable with the natural variation, this procedure does not cause any loss in accuracy. The experimental configuration is shown in figure 4. The phototransistors (PT's) are used to detect if the amplitude on the screen is greater than the PT position. Although the transistors have lenses of 3 mm diamter they trigger if the edge of the laser spot reaches the edge of the lens. The accuracy in amplitude is thus limited to the accuracy in measurement of the PT position, typically $\pm$ 0.25 mm to $\pm$ 0.5 mm. The positions of the phototransistors were chosen to give roughly equal intervals in $\ell n\theta$.

θ is calculated from

$$\tan(\theta+\delta\theta) = \frac{x}{d}$$

The screeen is perpendicular to the laser beam to $\lesssim 1^{o}$, a negligible error. The zero error is calculated from the time spent by the laser beam to the left

and right of the central PT for a given amplitude, θ_m

$$\frac{\delta\theta}{\theta_m} = \cos\left(\frac{T_R\pi}{T_L+T_R}\right)$$

so

$$\delta\theta = \frac{\cos\left(\frac{T_R\pi}{T_L+T_R}\right)\ \tan^{-1}(x_m/d)}{1+\cos\left(\frac{T_R\pi}{T_L+T_R}\right)} \qquad (22)$$

The centre phototransistor can also be used for measuring the period of the oscillation.

Figure 5 and 6 are schematic diagrams of the circuit used. Figure 7 and 8 show the details of the major sections of the circuits (i.e. details of displays etc. are omitted). An IC list and pinouts are given in the appendix.
The operation of the circuit is as follows: the PT's are connected to a trigger (555) which produces a voltage pulse of a few tenths of a second duration. This gives reliable triggering and also drives an LED for a visual check on the triggering. The central PT drives a 3 digit BCD counter via a divide by two (JK flip flop). PT0 resets the counter, and PT 1 to PT 4 update the corresponding displays to the current state of the counter. Thus each display is updated until the laser beam just fails to reach the PT, and the count is then frozen. A "master latch enable" (MLE) output is derived from PT4 to freeze the display a couple of minutes after the last pulse from PT 4 (i.e. at the end of a run). This prevents any spurious signals causing a loss of data if the system is left for some time. The start button puts MLE high and also triggers the starter circuit.

The timing circuitry operates in one of two modes, zero position or period. In the zero position mode the time spent to the RHS and LHS of PTC are measured by enabling two 6 decade counters for an appropriate interval. The counters are clocked at 10kHz(nom.) by a 555, giving timing to 0.1 ms.

In period mode succesive periods are measured on alternate displays, each counter being reset after the display has been held for half a cycle. An output is available for calibration of the clock frequency, if required.

In zero position mode the counters are reset by one of PT0 to PT 4, to give a measurement at a particular amplitude.

The counters drive multiplexed displays via buffer transistors; the strobe output is also used to strobe the common cathode of the displayed counts to give similar brightness.

Various sources of error must be considered in measuring the log. dec. in this way. Firstly, consider errors in the calculated zero position. We have assumed θ_m constant, whereas it will change by $\sim \frac{1}{2}\%$ over one oscillation. Since $\delta\theta = \theta\cos\left(\frac{T_R}{T_L+T_R}\right)$ this gives $\sim \frac{1}{2}\%$ error in $\delta\theta$, or δx. As $\delta x \lesssim$ 5 mm typically, this error is negligible.

An error in the timing of T_L and T_R will arise from the finite size of the phototransistor; the timing sequence is indicated in figure 9. If $x \simeq a \sin \omega t$ $v \simeq a\omega \cos \omega t = \omega\sqrt{a^2 - x^2} \Rightarrow \frac{dv}{dx} = \frac{-\omega x}{a^2-\omega^2} \simeq -\frac{\omega x}{a} z$ at x_z as $x_z \ll a$. The timing error arises from the incorrect travel time across half of the pt, due to the difference in velocity over half the pt: i.e. $dt \sim \frac{1}{4}\left(\frac{dx}{V} - \frac{dx}{V+dv}\right)$

$$\sim \frac{1}{4}\frac{dxdv}{v^2}$$

$$\sim \frac{1}{4}\frac{dx_2\, x_z dx}{a\, v^2} \qquad (23)$$

$$\sim \frac{1}{4}\frac{x_z dx^2}{a^3\omega}$$

and with $x_z \sim 5$ mm

$dx \sim 3$ mm

$\omega \sim 1$

$a \sim 200$ mm

we get $dt \sim 1$ μs

which is quite negligible.

The effect of the finite laser spot size should be of a similar magnitude.

(The value for δx generally varies by a few tenths of a mm between runs, which can probably be attributed to small timing errors due to slight non-axial vibration of the disc). Secondly, a small correction due to the PMMA can be made to the amplitudes x_m (figure 10)

$$\delta = t \sin\theta \left(1-\frac{1}{N}\right) \qquad (24)$$

where N is the refractive index of PMMA = 1.495. δ ranges up to $\sim$ 0.7 mm for the $m = o$ position. Thirdly, the beam path on the screen is roughly parabolic due to the vertical inclination of the incoming beam.

The beam height at the screen is

$$H \simeq \left(1 + \tfrac{1}{2}\left(\frac{x}{d}\right)^2\right)H_o \qquad (25)$$

where H_o is the height of the beam at the central pt. This could give errors due to triggering at positions other than the edge of the PT. However, if H_o is minimised the maximum deviation, $H-H_o$, is only a few mm, and this can be compensated for by a small vertical displacement of the PT. Finally, the main cause of error, external vibration, must be considered. Although this cannot create a torque about the wire axis, if the non-axial vibration is sufficient to cause a few mm displacement at the screen there is a chance of slight inaccuracies in the counting. If the displacements are greater, then there is the possibility of missing a count. This is less important for PT O-PT 4 as they only need 1 in 2 "attempts" to suceed, and provided the final contact is made, i.e. when amplitude = position of PT, no error is introduced. For the centre PT, the high velocity of the spot seems to give better reliability. On the whole if the screen is set up correctly it is possible to keep vertical vibration amplitudes $\gtrsim$ 1 mm, and the circuit usually performs with 100% reliability. Measurements at low pressure can be more difficult, as the log. dec. for pendulum oscillations is also reduced. However, it is obvious from the results when a significant number of counts have been missed, and the log. dec. can be found "by hand".

5. Experimental Results

For each experiment the four numbers and two times recorded by the automatic circuitry are fed into a Hewlett Packard HP41CV programmable calculator. This calculates, and corrects for, the zero position error and then performs a least square regression of the counts (including count 0) on the natural logarithm of the angular amplitudes.

Both Δ and the goodness of fit are calculated. Sample results are given below (zero position calculated using PT 2)

36 Gauge Piano Wire				38 Gauge Cu/Be Wire			
counts	96	192	289 387	74	149	223	297
T_L and T_R	2.3255		2.3810	5.5289		5.6082	

The parameters calculated from these figures are:-

$\delta_x = -6.04$ mm	$\delta_x = -3.62$ mm
$\Delta = 0.004099$	$\Delta = 0.005341$
$r^2 = 0.999985$	$r^2 = 0.999996$

(see figures 11 and 12)

In a series of several measurements Δ can typically be determined to $\simeq 0.1$ %, this is of the desired order of accuracy.

A series of measurements on air at various pressures and at $20.05 \pm 0.05^{o}C$ has been performed.

The specifications of the wire and disc used are as follows:

Disc

m = 47.15 g
R = 42.49 mm
h = 1.00 mm
centre hole 3 mm radius (OBA clearance)

$I = 4.28 \times 10^{-5}$ kgm^2 (not corrected for pinchuck; not an appreciable error).

Wire

Cu/Be

d = 0.148 ± 0.001 mm
l = 16 cm

$E = 1.17 \times 10^{11}$ Pa (ref. 14)
$\sigma = 0.35$ (ref. 14)

The viscometer was set up with

$b_1 = 9.5$ cm
$b_2 = 21$ cm
$b_3 = 5$ cm
} to nearest 0.5 cm

$d = 1820 \pm 10$ mm
$X_o = 750.0$ mm
$X_1 = 488.5$ mm
$X_2 = 323.0$ mm
$X_3 = 214.5$ mm
$X_4 = 143.0$ mm
} to nearest 0.5 mm; corrected for perspex

In leak measurements the viscometer was found to leak from vacuum at a rate of ~ 0.02 mbar/hour. The measured period was 11.27 s. Equation 5 leads to a value of 11.5 ± 0.3 s. The results of the tests are presented in figure 13 with the wire damping, Δ_o, taken as 0.00045 ± 0.00005.

It can be seen that there is very good agreement between experiment and equation 19, within the region of validity of the equation. At lower pressures equation 20 gives the correct viscosity dependence. Below 1 mbar the logarithmic decrement appears to fall again although the results showed some irreproducibility. This could be due to slip, effusion of lighter gases into the system or an actual change in viscosity. This is to be investigated; a slip or viscosity change seems unlikely as the mean free path is no more than a few mm (see Kennard[5]).

Generally, the results indicate that the theory of the viscometer is adequate and that it can be used to measure viscous drags over a wide range of gas pressure.

6. Comments on the Experimental Results of Kestin and Shah

The results of Kestin and Shah generally showed few significant changes in viscosity. The most significant changes were observed at low pressure, with a disc that was calibrated, removed and coated with $^{210}P_o$ (an α emitter) and

replaced in the viscometer. Slight increases in damping were observed for most gases, but a reduction of 7.6 % in apparent viscosity was observed for air at 1 mmHg.

As at most a few measurements were made for each gas, the magnitude of the error was uncertain, but probably was of a few %. This means the increases are not at a high confidence level. There is also the possibility of a change in calibration having occured. Another problem is that the pressure varied by up to several percent between the radioactive and inactive measurements. For example, there was a 5% decrease in the density of the air for the 1 mm Hg measurements. Since the viscometer may have been operating in a pressure dependent regime (cf figure 13) this might have been a significant error.

In the other case of significance, Argon at 1 atmosphere, a +5.2% change was observed, with a 1% increase in pressure.

7. Conclusions and Future Work

A very accurate viscometer has been developed and built to measure small viscosity changes over a range of pressures. Our initial measurements together with an analysis of Kestin and Shah's work suggest that air and argon should be studied over a range of pressures, the low pressure measurements being conducted in the pressure independent regime. A more accurate theory of the low pressure behaviour should also be developed. To investigate possible chemical effects on irradiation measurements should be made with inert gases and with gas mixtures containing potentially reactive gases such as ethylene. An investigation of the effect of water vapour concentration would also be of interest.

REFERENCES

1. Clark, J., Kestin, J. and Shah, V.L., The Effect of Long Range Intermolecular Forces on the Drag of an Oscillating Disc and on the Viscosity of Gases, Physica 89A (1977) pp539-554.
2. Clark, J., Field, J.E. and Wilby, W.A., Interim Scientific Report No.1, 1980.
3. Davies, B., Integral Transforms and their Applications, Springer-Verlag, 1978.
4. Field, J.E., Wilby, W.A., Rees, W.G. and Clark, J., Interim Scientific Report No.2 1981.
5. Kennard, E.H., Kinetic Theory of Gases, McGraw-Hill, 1938.
6. Kestin, J. and Wang, H.E., Corrections for the Oscillating Disc Viscometer J. Appl. Mech. 24 (1957)$_p$197.
7. Kestin, J. and Shah, V.L., AFFDL-TR-68-86.
8. Landau and Lifshitz, Theory of Elasticity, Pergamon.
9. Lebedev, N.N., Special Functions and Their Applications, Prentice Hall, 1965.
10. Mariens, P., van Paemel, O., Theory and Experimental Verification of the Oscillating Disc Method for Viscosity Measurements in Fluids, App. Sci. Res. 5 (1956)p 411.
11. Schlichting, H., Boundary Layer Theory 7th ed., McGraw-Hill (1979).
12. Sparrow, E.M. and Gregg, J.L., Mass Transfer, Flow and Heat Transfer about a Rotating Disc, Trans. ASME J. Heat Transfer 82 (1960)pp 294 - 302.
13. Stokes, G.G., On the Effect of the Internal Friction of Fluids on the Motion of Pendulums, Cambr. Phil. Trans. IX, 8(1851) p 8.
14. Tennent, R.M. (ed), Science Data Book, Oliver and Boyd, 1971.
15. Wilby, W.A., Studies of Aerodynamic Drag, C.P.G.S. Dissertation, University of Cambridge, 1980.

Appendix

IC List and Pinouts

TIL 313	7 Segment LED display
555	Timer
4001	Quad 2i/p NOR
4002	Dual 4i/p NOR
4011	Quad 2i/p NAND
4016	Quad Switch
4027	Dual JK Flip Flop
4069	Hex NOT
4070	Quad 2i/p EX-OR
4510	BCD Counter
4511	BCD 7 Segment Display Driver
50395	Six Decade Counter/Display Driver

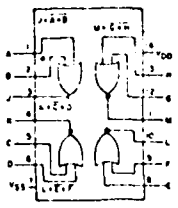

4001BE

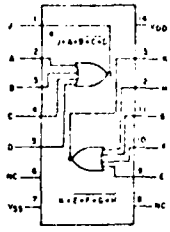

4002BE

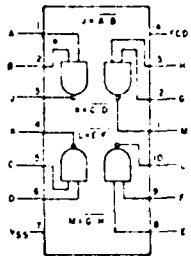

4011BE

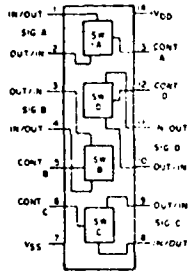

4016BE

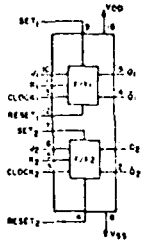

4027BE

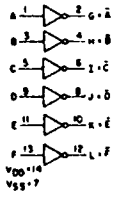

4069UBE

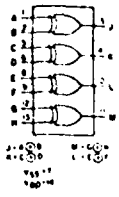

4070BE

555 timer

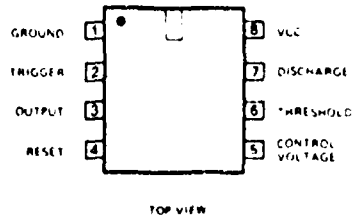

TOP VIEW

TIL 313 DISPLAY

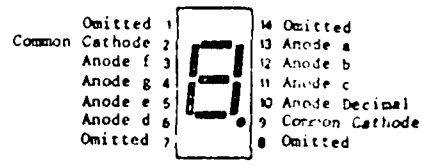

4510

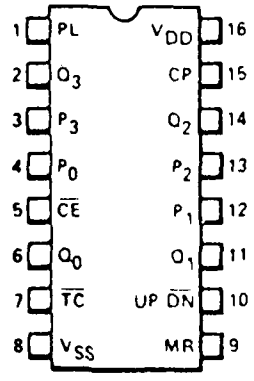

PL	Parallel Load Input (Active HIGH)
P_0-P_3	Parallel Inputs
$\overline{CE}$	Count Enable Input (Active LOW)
CP	Clock Pulse Input (L → H Edge-Triggered)
Up/$\overline{Dn}$	Up/Down Count Control Input
MR	Master Reset Input
$\overline{TC}$	Terminal Count Output (Active LOW)
Q_0-Q_3	Parallel Outputs

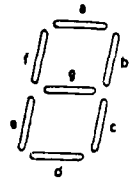

4511

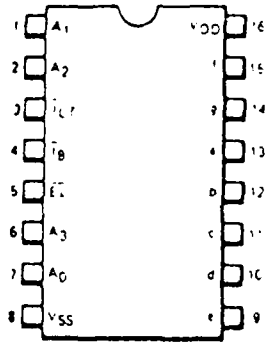

A_0- A_3	Address (Data) Inputs
$\overline{EL}$	Latch Enable (Active LOW) Input
$\overline{I_B}$	Blanking (Active LOW) Input
$\overline{I_{LT}}$	Lamp Test (Active LOW) Input
a-g	Segment Outputs

MK50395 SIX DECADE COUNTER/DISPLAY DRIVER

A six decade synchronous up/down counter and display driver with a compare register and storage latches. The counter features look-ahead carry or borrow and multiplexed BCD and seven segment outputs with direct LED segment drive and leading zero blanking. Connect a 330pF capacitor between pins 21 and 1, +12V DC to pin 1 and ground to pin 22.

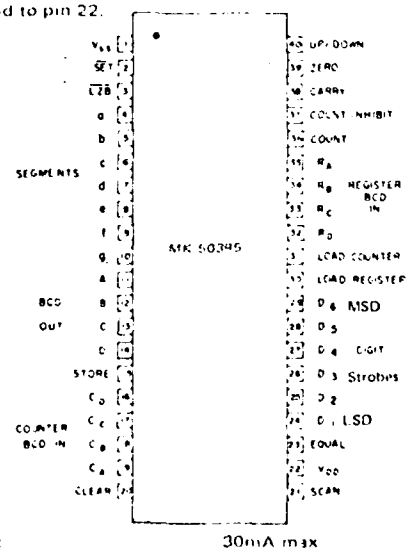

Supply current:	30mA max
Output current digit strobes:	3mA max
segment outputs:	10mA max
Count input frequency:	1MHz max

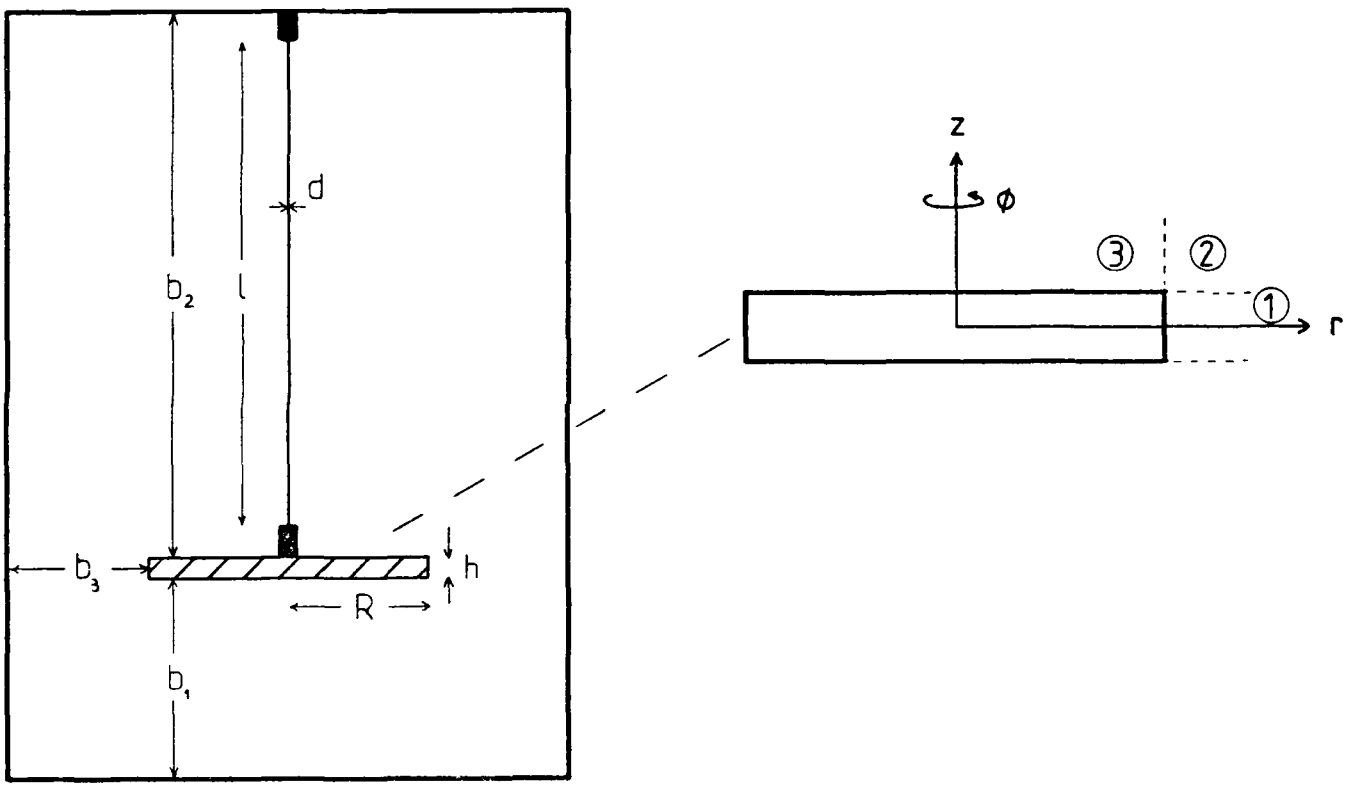

Fig. 1. Schematic Diagram of Viscometer.

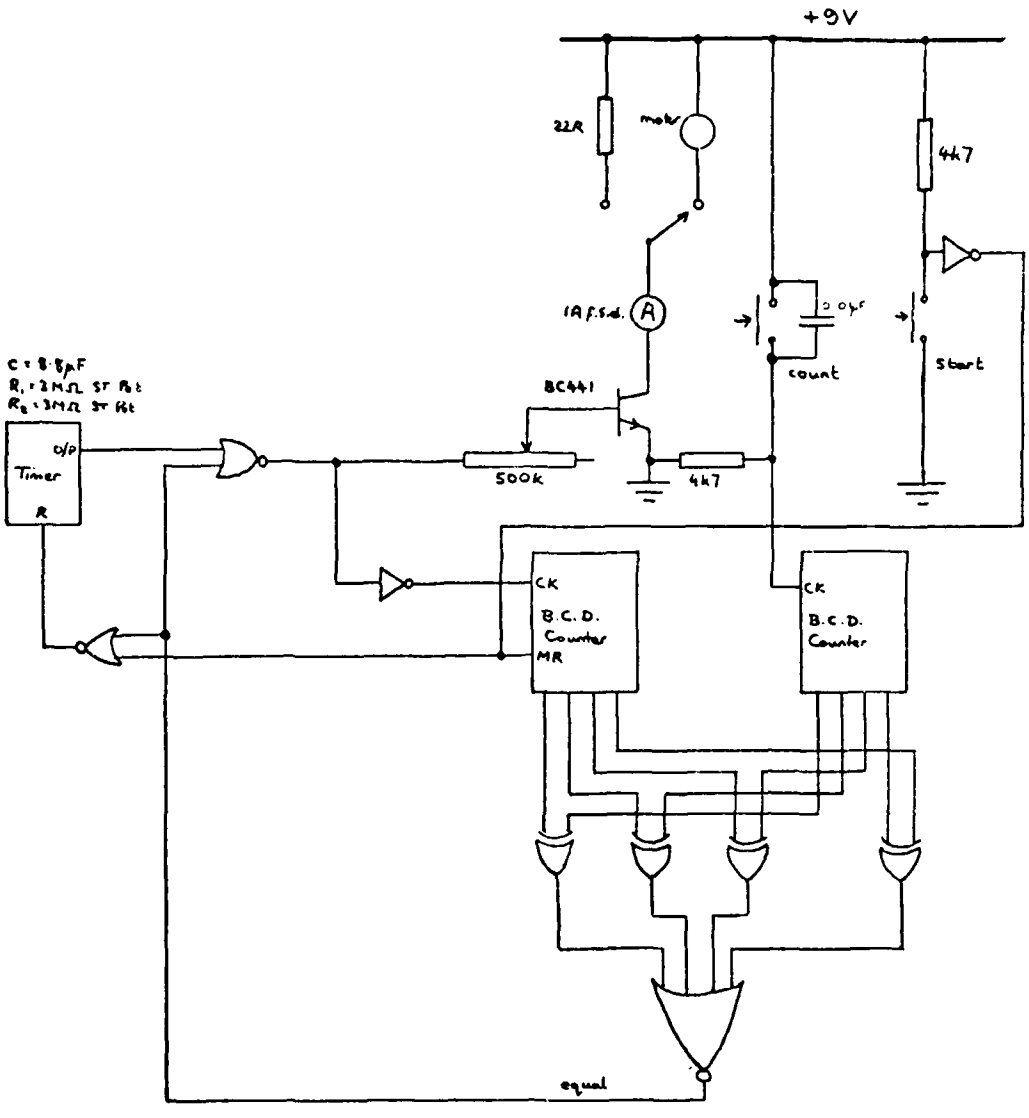

Fig. 2. Schematic Diagram of Starter Circuit.

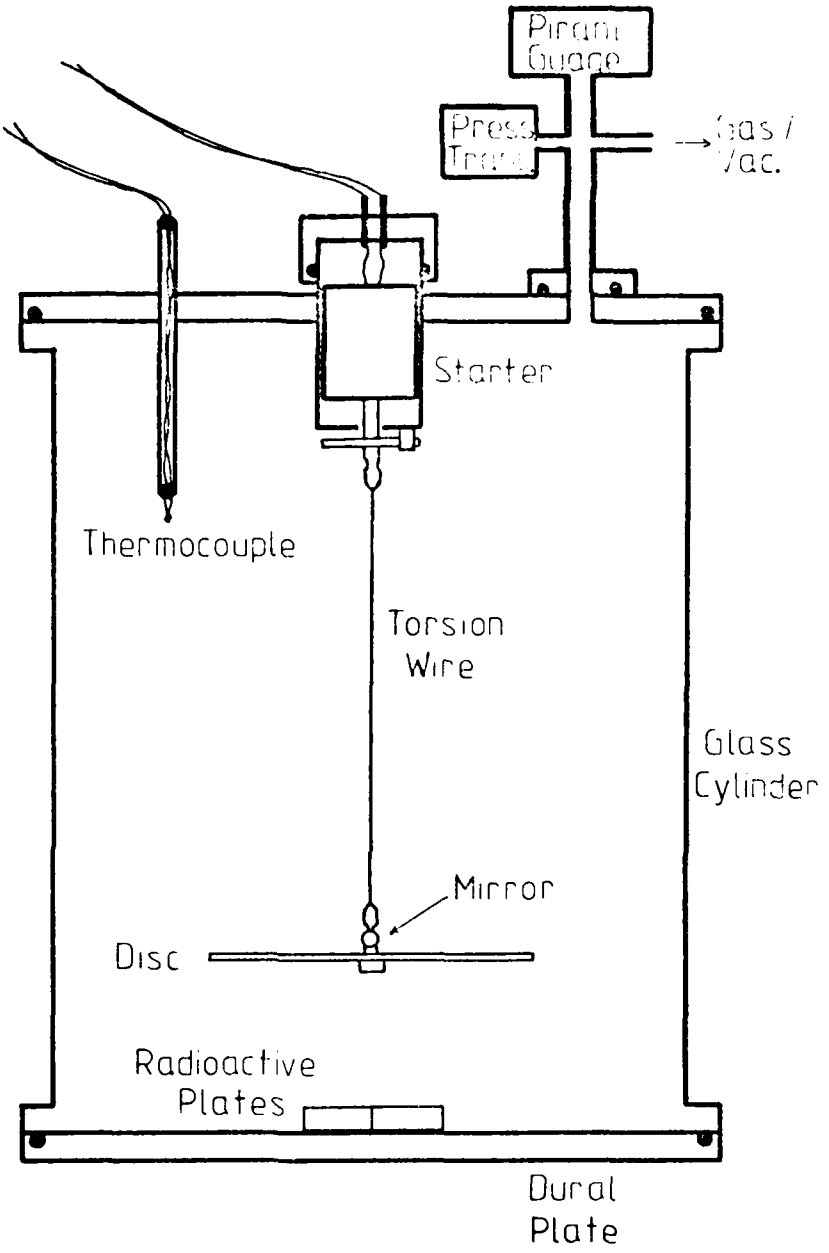

Fig. 3. Torsion Disc Viscometer.

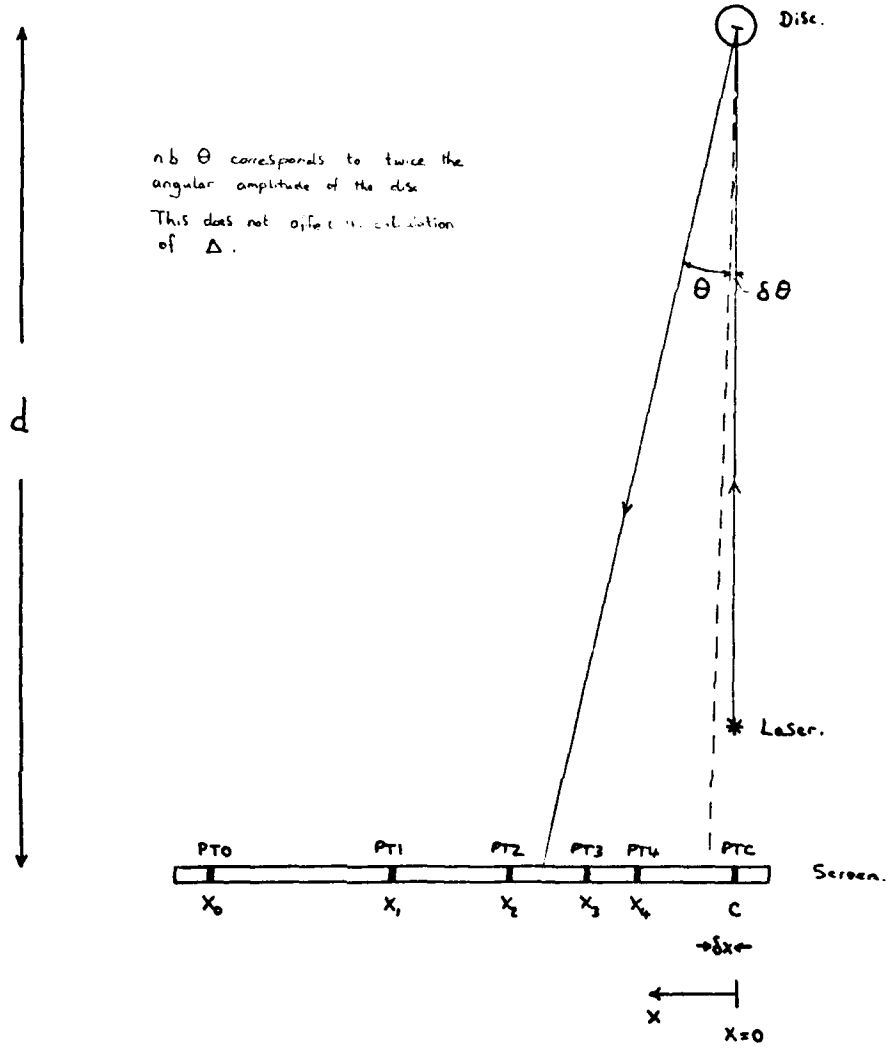

Fig. 4. Experimental Configuration.

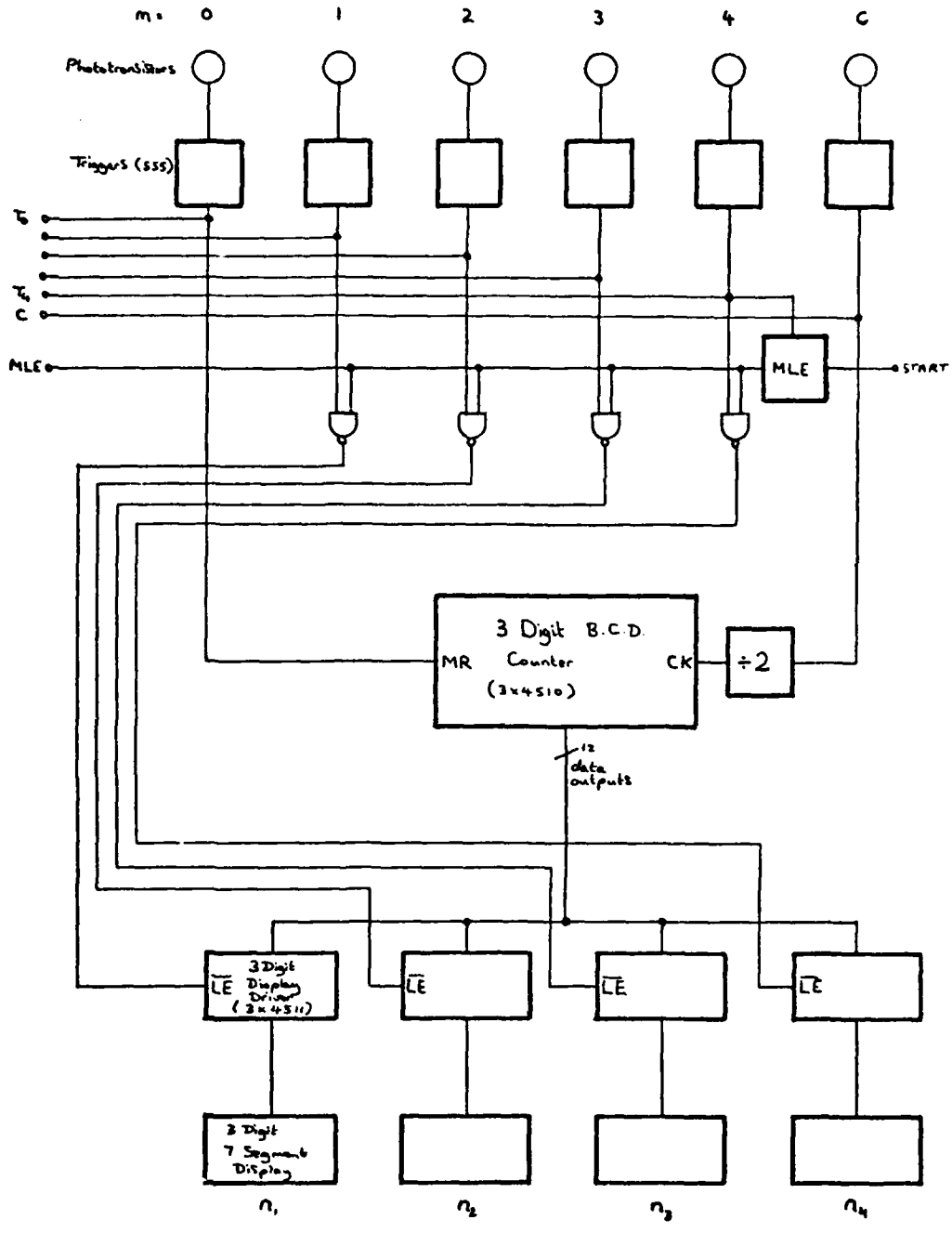

Fig. 5. Schematic Diagram of Data-Logging Circuit :- Counters.

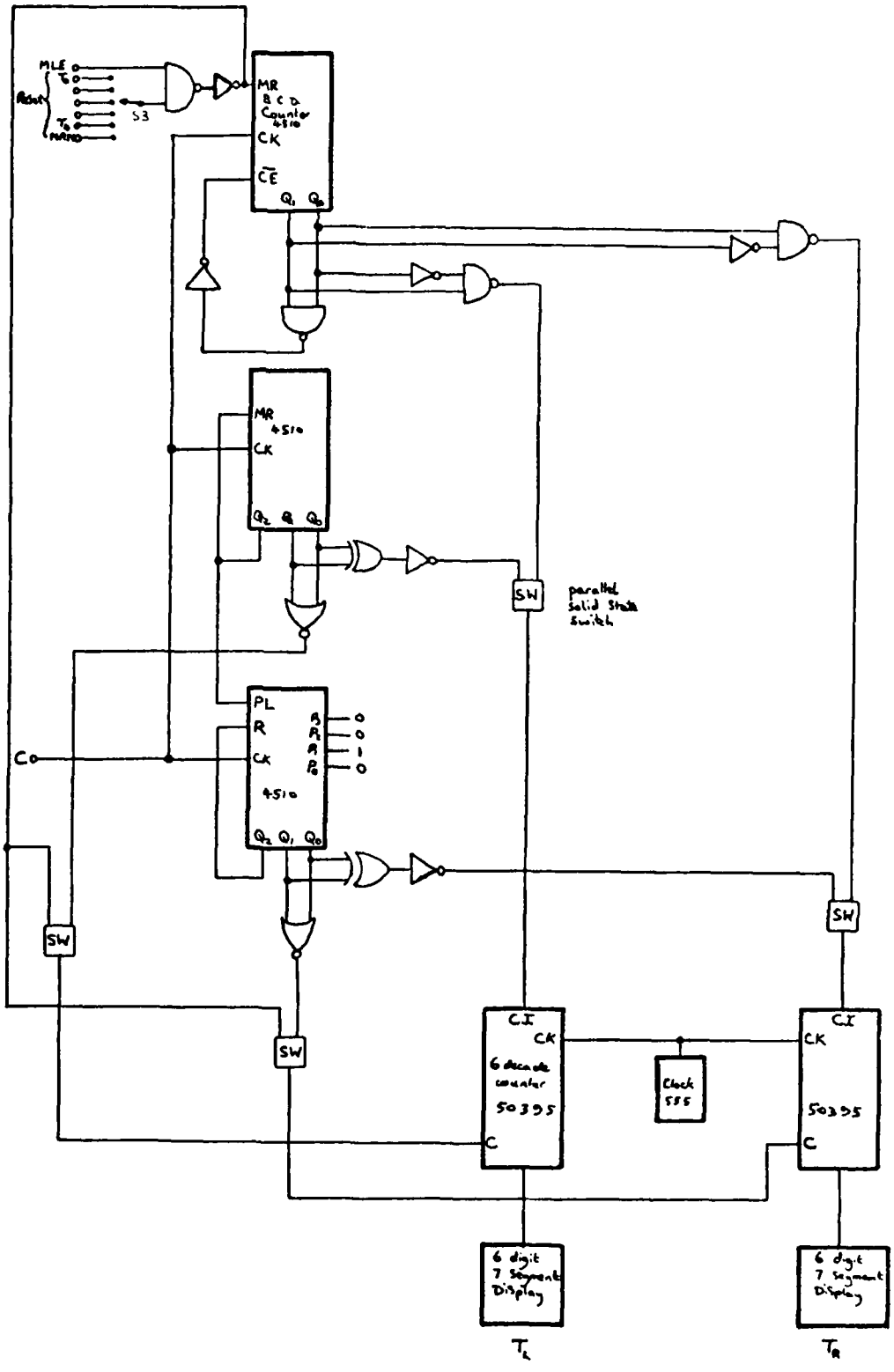

Fig. 6. Schematic Diagram of Data - Logging Circuit :- Timers .

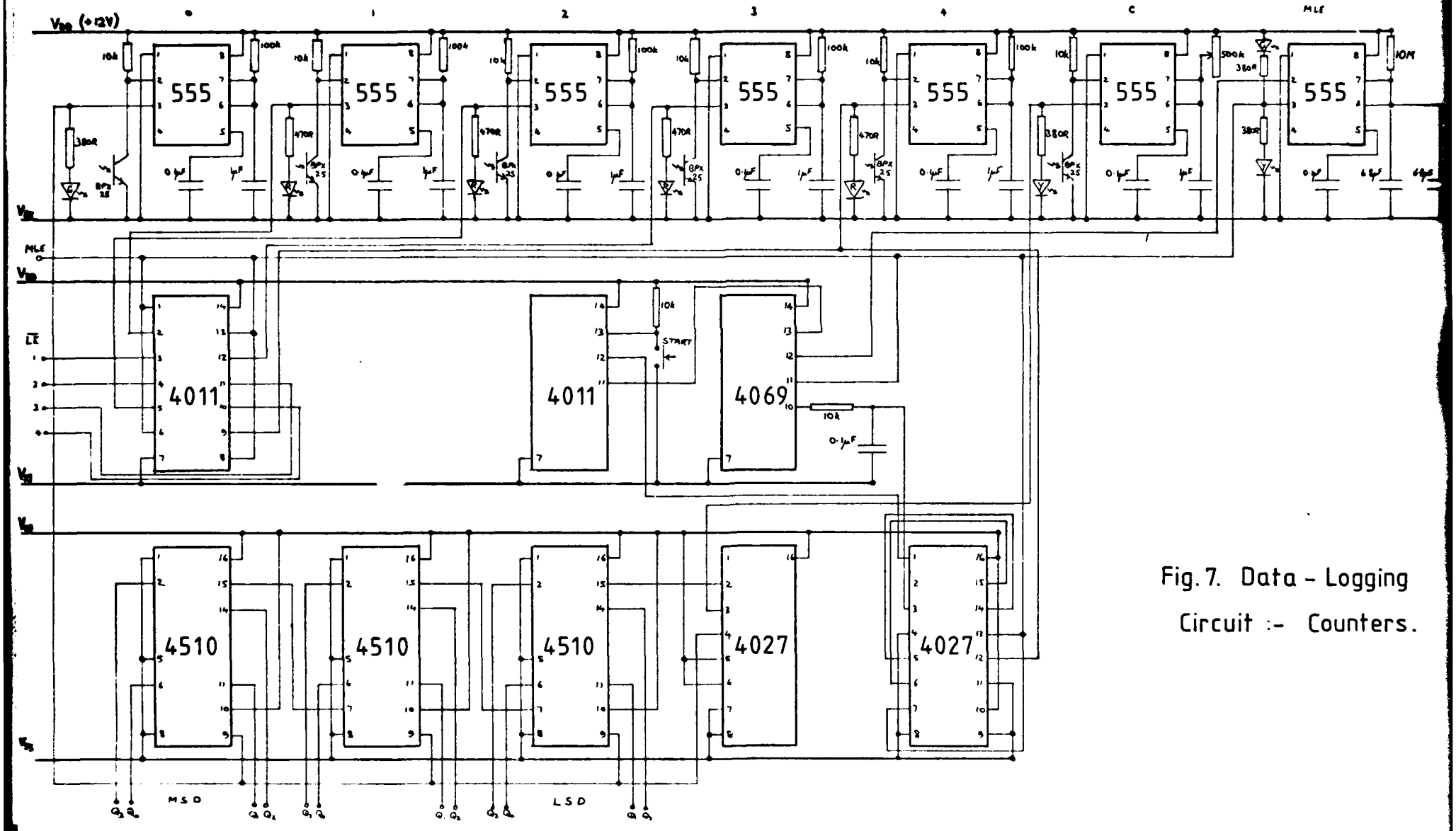

Fig. 7. Data - Logging Circuit :- Counters.

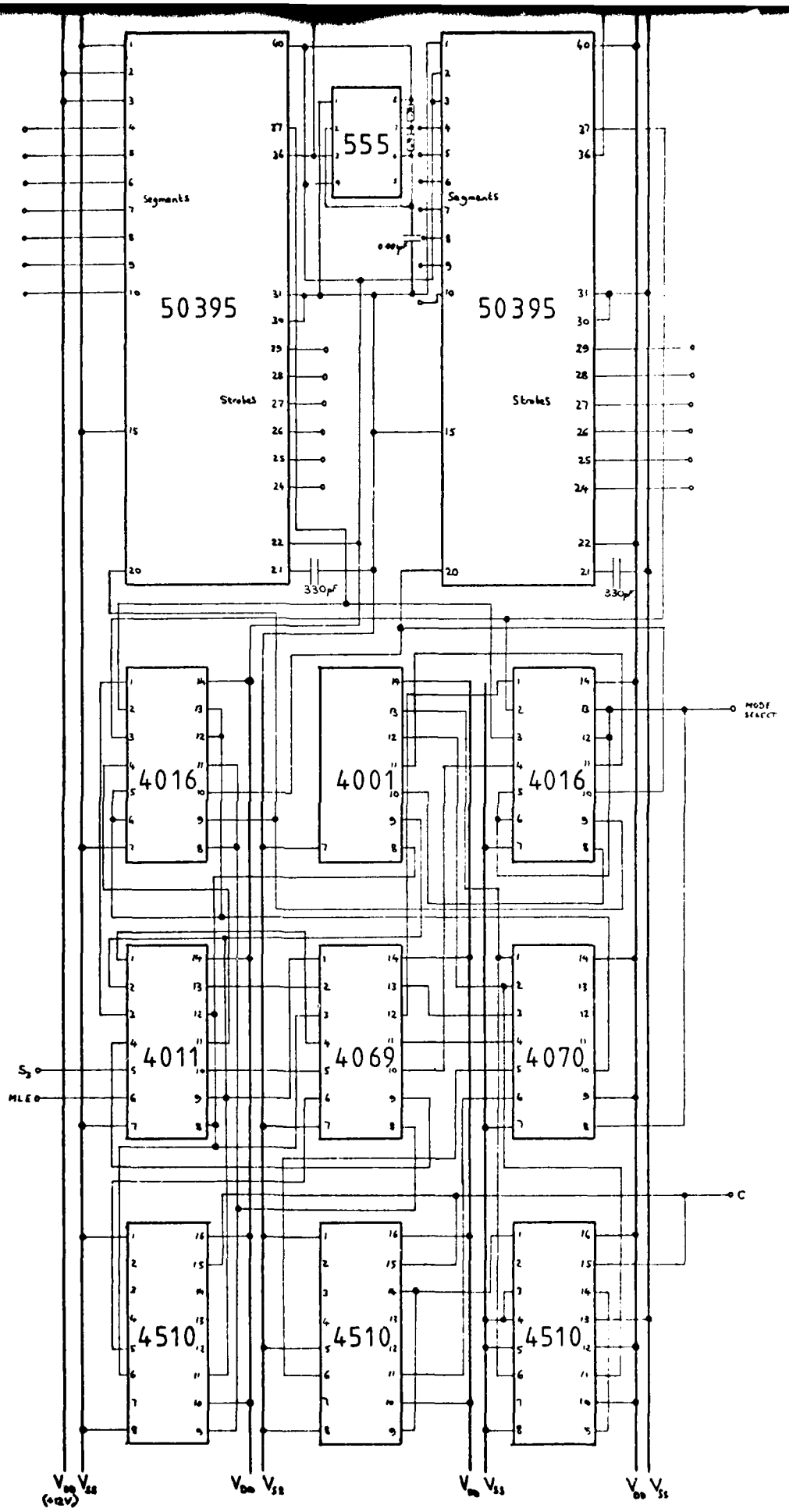

R_1 & R_2
500 kΩ pots
adjusted to give
f = 10 kHz

Fig. 8. Data - Logging Circuit :- Timers.

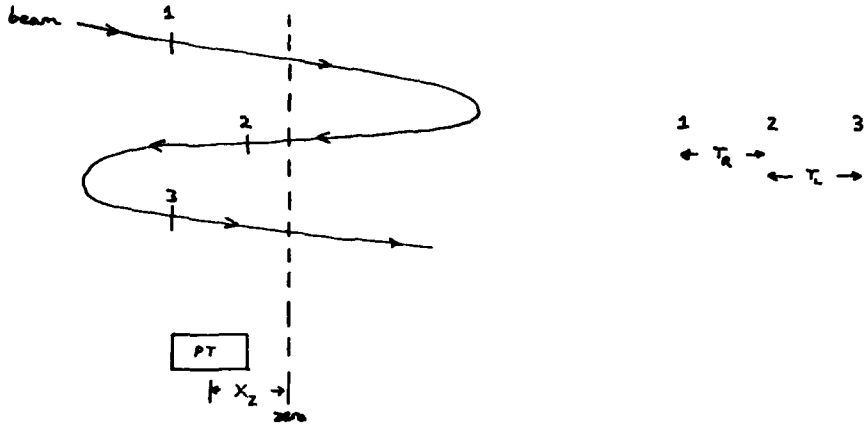

Fig.9. Zero Position Timing Sequence.

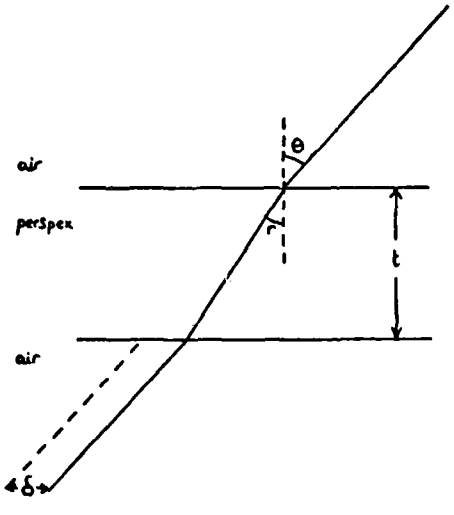

Fig.10. Correction for Perspex (PMMA).

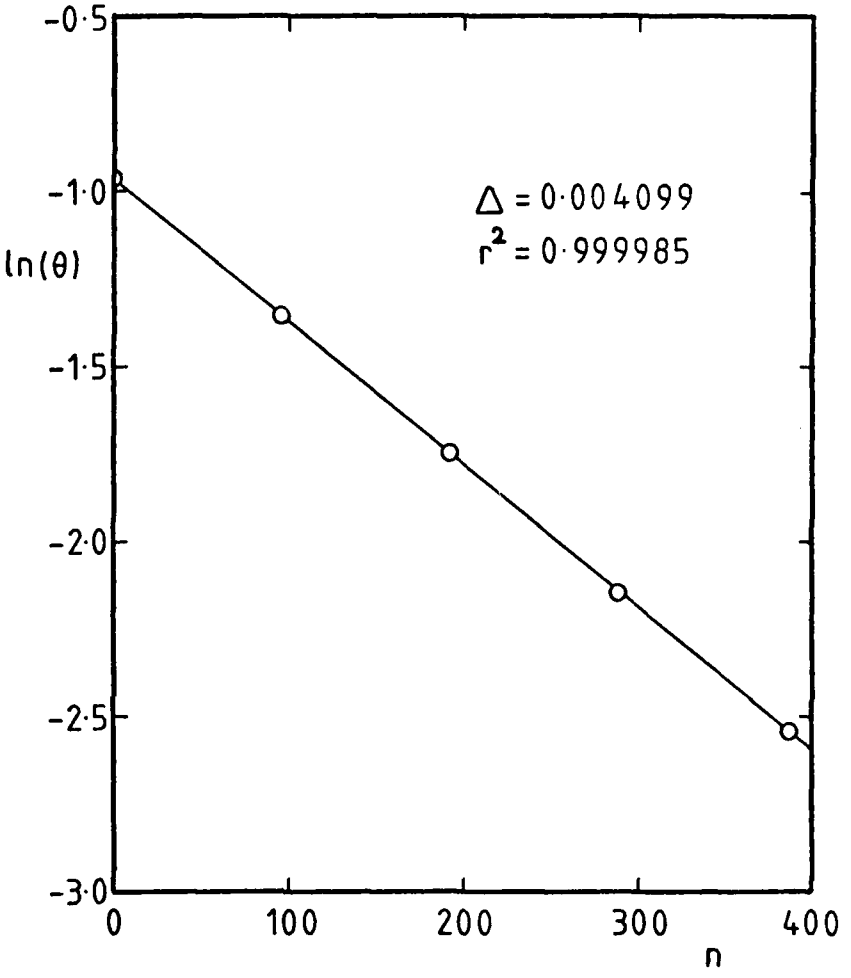

Fig. 11. Typical Decay Curve, Steel Torsion Wire.

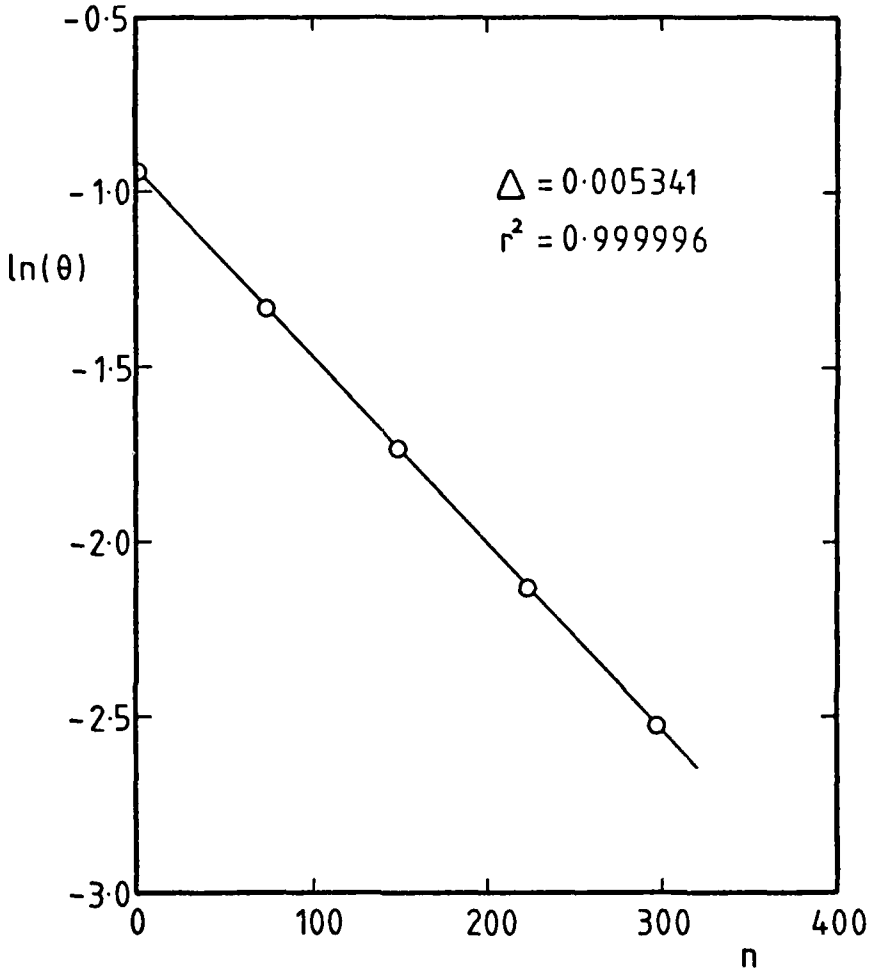

Fig. 12. Typical Decay Curve,
Cu/Be Torsion Wire.

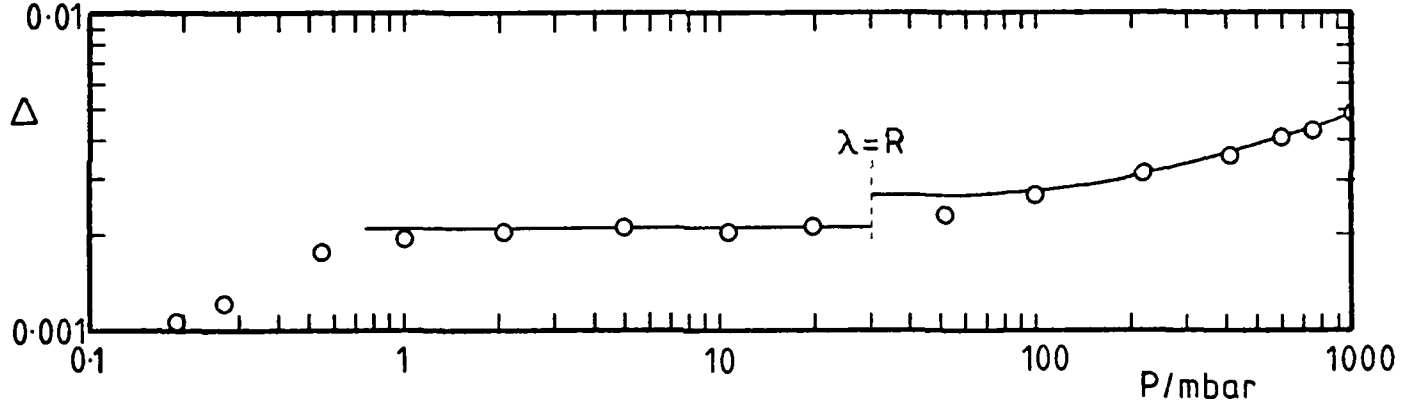

Fig.13. Logarithmic Decrement vs Pressure, for Air.


FILMED
8-8